# physica status solidi pss

www.interscience.wiley.com

*reprints*

www.pss-rapid.com

www.pss-c.com

www.pss-b.com

www.pss-a.com

WILEY-VCH

WILEY InterScience® DISCOVER SOMETHING GREAT

EarlyView publication on www.interscience.wiley.com
(issue and page numbers not yet assigned;
citable using Digital Object Identifier – **DOI**)

Phys. Status Solidi B, 1–6 (2009) / **DOI** 10.1002/pssb.200945531

physica status solidi pss b
www.pss-b.com
*basic solid state physics*

# Structure and luminescence of rare earth-doped silicon oxides studied through their X-ray absorption near edge structure and X-ray excited optical luminescence

**Editor's Choice**

**T. Roschuk*, P. R. J. Wilson, J. Li, O. H. Y. Zalloum, J. Wojcik, and P. Mascher****

Department of Engineering Physics and Centre for Emerging Device Technologies, McMaster University, 1280 Main St. W, Hamilton, Ontario L8S4L7, Canada

Received 9 August 2009, revised 22 October 2009, accepted 23 October 2009

**PACS** 78.55.Qr, 78.70.Dm

---

* Corresponding author: e-mail roschutr@mcmaster.ca, Phone: +1 905 525 9140 x26196, Fax: +1 905 527 8409
** e-mail mascher@mcmaster.ca

The X-ray absorption near edge structure (XANES) and X-ray excited optical luminescence (XEOL) of a set of photoluminescent rare earth (RE) (Tb, Ce) doped silicon oxide ($SiO_x$) thin films, having compositions ranging from O-rich (32% Si) to Si-rich (36% Si), were analyzed at the Si and O *K*-edges. The results show that luminescence from these materials is correlated with the excitation of O-related energy states, and demonstrate that the composition and bonding structure of the silicon oxide host matrix play an active role in determining the luminescent properties of these materials, although the microstructure of the films may vary from film to film.

**1 Introduction** Light emission from Si-based materials has been of significant interest over the past several years due to the enormous potential of a Si-based light source in integrated photonics [1, 2]. Two promising candidate materials that have been extensively explored are nanostructured Si, including porous Si and Si-nanoclusters (Si-ncs), and rare earth (RE) doped silicon-based materials [3–5]. The emission of the $Er^{3+}$ ion at 1.54 μm has made it by far the most extensively studied of the RE-dopants due to the applications of its emission in the area of telecommunications [6–8]. More recently, there has been a growing interest in the use of Si-based materials in areas outside of integrated photonics, such as solid state lighting (SSL) or displays, which could gain significant competitive benefits from the large infrastructure and low-cost available to the Si microelectronics industry [9]. In order to implement Si-based SSL it is necessary to consider the luminescence of other RE ions which emit in the visible and can be used for color mixing in order to generate white light. Specifically, Ce, Tb, and Eu have the blue, green, and red emissions, respectively, necessary for such applications and have previously found extensive use in phosphor-based displays. The luminescent properties of Si-based materials doped with these RE elements have only been lightly studied, focusing on the fabrication of electroluminescent devices [10–12]. Details of the physical mechanisms involved in the luminescent process remain largely unstudied. In the case of Er-doped silicon oxides, it has been demonstrated that the luminescence efficiency is increased by the presence of Si-ncs, formed in Si-rich silicon oxides (SRSOs) through thermal annealing. In such a case, the Si-ncs act as sensitizers to the $Er^{3+}$ ion. In the case of RE-dopants with emission in the visible it is not clear that the bandgap of the Si-ncs is sufficiently wide to excite the RE ions, particularly in the cases of Ce and Tb. Furthermore, recent results have shown that bright luminescence is observed in Ce- and Tb-doped samples where the silicon submatrix was an oxygen-rich silicon oxide (ORSO) [13].

In this paper we discuss the analysis of Tb- and Ce-doped silicon oxides through the study of their X-ray absorption near edge structure (XANES) and X-ray excited optical luminescence (XEOL), both of which have previously been applied to the study of luminescent Si-based materials [14–17]. The site-specific nature of the XEOL process indicates that the luminescence of these materials is strongly correlated with O-related energy states in both SRSO and ORSO Tb-doped thin films and in a Ce-doped ORSO thin film, although the microstructure varies from film to film.

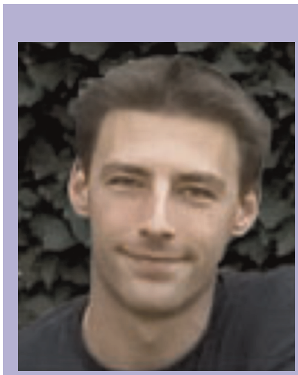

**Tyler Roschuk** completed a B.Sc. in Engineering Physics at the University of Saskatchewan (Canada) in 2002, and MA.Sc. and Ph.D. degrees at McMaster University in 2005 and 2009, respectively. He is currently employed as a research associate at McMaster University in Peter Mascher's research group. His research interests are in the fabrication and characterization of nanostructures and quantum materials for applications in nanophotonics, nanoelectronics, and plasmonics. In January 2010 he will start a post-doctoral fellowship at Imperial College London (UK) studying the design of plasmonic nano-antennae coupled to quantum materials in the research group of Stefan Maier.

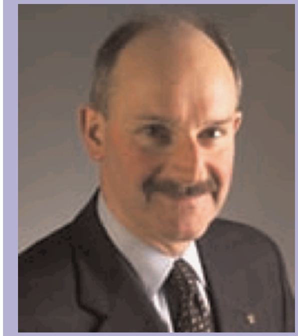

**Peter Mascher** obtained a Ph.D. in Engineering Physics from the Graz University of Technology (TUG) in Austria. He joined McMaster University in 1989, is a professional engineer and a professor in the Department of Engineering Physics, and currently serves as the Associate Dean (Research and External Relations) of the Faculty of Engineering. Dr. Mascher is a member of McMaster's Brockhouse Institute for Materials Research and the Centre for Emerging Device Technologies. In 2001, he was appointed (and re-appointed in 2006) as the inaugural holder of the William Sinclair Chair in Optoelectronics. Dr. Mascher leads active research groups involved in the fabrication and characterization of thin films for optoelectronic applications, the development and application of silicon-based nanostructures, and the characterization of defects in solids by positron annihilation spectroscopy. As a member of the executive body of the Dielectric Sciences and Technology Division of the Electrochemical Society, he has led and organized several international symposia on the 'Science and Technology of Dielectrics for Active and Passive Devices' and on 'Nanocrystal Embedded Dielectrics for Electronic and Photonic Devices'.

## 2 Experimental

### 2.1 Thin film deposition and processing

Rare earth-doped silicon oxide thin films with thicknesses from 70 to 110 nm were grown on ⟨100⟩ Si substrates by electron cyclotron resonance plasma enhanced chemical vapor deposition. The silicon and oxygen precursors were silane (30% $SiH_4$ in Ar) and $O_2$ (10% $O_2$ in Ar), respectively. The volatile metal organic compounds $Tb(tmhd)_3$ or tris (2,2,6,6-terametyl-3,5-heptanedionato)-Tb(III), and $Ce(tmhd)_3$ or tris (2,2,6,6-terametyl-3,5-heptanedionato)-Ce(III) were used as the Tb and Ce precursors, respectively. The RE sources were heated to 200 °C within a manifold to sublime the precursor and introduced into the chamber alongside the silane using Ar as carrier gas. During the deposition process the substrate stage was heated to a temperature of 350 °C, resulting in a surface temperature of the sample of 120 °C. Substrate rotation was used to achieve uniformity and homogeneity of the films. Sample compositions were determined by Rutherford backscattering spectrometry performed at the University of Western Ontario. The Si and Tb concentrations of the samples were as follows: Tb-doped ORSO ($32 \pm 2\%$ Si, $0.40 \pm 0.03\%$ Tb), Tb-doped SRSO ($36 \pm 2\%$ Si, $0.30 \pm 0.02\%$ Tb), and Ce-doped ORSO ($32 \pm 2\%$ Si, $0.90 \pm 0.06\%$ Ce). Post-deposition, the samples were cleaved and annealed at temperatures from 700 to 1200 °C in a quartz tube furnace under flowing $N_2$. Further details of the deposition system, film growth, and structure have previously been discussed [13, 18, 19].

### 2.2 Photoluminescence

Conventional photoluminescence of the samples was excited by a HeCd laser emitting at 325 nm. The photoluminescence spectra were measured using an Ocean Optics spectrometer and corrected for system response [20].

### 2.3 Soft X-ray-based spectroscopy studies

X-ray absorption near edge structure and X-ray excited optical luminescence measurements were performed at the Canadian Light Source (CLS) synchrotron facility using the 11ID-1 spherical grating monochromator to access the different elemental absorption edges of the constituent atoms [21, 22]. The incident X-ray beam was scanned across the relevant edge energies in steps of 0.1–0.5 eV, with the finer step size being used over the edge and peak regions of interest and the larger step size being used in the pre- and post-edge regions. At each excitation energy, the total electron yield (TEY), which is proportional to X-ray absorption by the sample, was measured with a 1 s integration time and a XEOL spectrum was recorded using an Ocean Optics QE65000 spectrometer. The photoluminescence yield (PLY) was then obtained by integrating the XEOL spectrum.

At the *K*-edge Si has an attenuation length of ~1.3 μm, however, the escape depth of electrons contributing to the TEY has been experimentally determined to be only ~100 nm [23]. This is on the order of the thicknesses of the samples grown for this work, resulting in the large Si–Si signal in the XANES at this edge. While the attenuation length of the PLY is substantially larger, no luminescence is excited in the Si substrate and thus the substrate does not contribute to the PLY signal. With the exception of the native oxide on the substrate surface no O is expected within the substrate itself. The TEY and PLY at the O *K*-edge, therefore, reflect only interactions occurring within the film layer.

**3 Results and discussion** Details of the growth, photoluminescence, and structure of Tb- and Ce-doped SRSO and ORSO thin films have previously been discussed [13, 18]. Of particular interest is that bright luminescence has been observed from a set of Tb- and Ce-doped samples in which the silicon oxide host matrix was oxygen rich. The luminescent behavior of the Tb-doped films is summarized in Fig. 1. For the SRSO films, high temperature ($T > 900$ °C) annealing is needed to induce Si-nc formation and attain luminescence. After annealing at 1100 °C a broad near-IR emission, attributable to Si-ncs, is observed. The sharp emission lines characteristic of the Tb$^{3+}$ ion are only clearly observed after a 1200 °C anneal. The appearance of the Tb$^{3+}$ emission lines is accompanied by the disappearance of the broad, near-IR emission from the Si-ncs. In contrast, luminescence is observed from Tb-doped ORSO films, both "as-grown" and at lower anneal temperatures, as is shown in Fig. 1b. Anneal temperatures greater than 700 °C have been found to lead to a decrease in the PL intensity of these films, with a rapid decrease in the integrated PL intensity being observed after annealing at temperatures above 800 °C. For Tb incorporated into a silicon oxynitride matrix it has been suggested that excitation of the luminescent Tb$^{3+}$ ion occurs through extended states of the host matrix followed by recombination through the Tb$^{3+}$ ion [24]. Such a scenario is unlikely for the case of Tb-doped silicon oxides, however, as the bandgap of the host matrix exceeds the typical excitation energies used for photoluminescence studies.

The TEY and PLY XANES spectra at the Si *K*-edge for the Tb-doped ORSO film are shown in Fig. 2a. Two key features are seen in the TEY spectra, a shoulder at 1839–1840 eV related to Si–Si bonding and an intense peak at 1847 eV which is a well-known feature of Si–O bonding corresponding to Si coordinated with four surrounding O atoms [25]. The Si–Si shoulder at 1839 eV is attributed to the substrate due to the small thicknesses of the films rather than to Si–Si bonding within the film itself, as the film thickness is comparable to the escape depth of electrons within SiO$_2$ [23]. While a weak Tb-related luminescence is observed at this edge in the XEOL spectra (inset) it is approximately of the same intensity as that observed after excitation in the pre-edge region at 1835 eV and is due to residual background absorption by the sample. At the Si–O related peak position, a strong resonant luminescence is seen in the PLY spectra. XEOL spectra at this energy illustrate that the luminescence corresponds to emission from Tb$^{3+}$ ions in both the as-grown and annealed samples, demonstrating that Tb luminescence is excited through O-related energy states. In order to confirm the excitation of Tb$^{3+}$ at oxygen related energies, the TEY and PLY XANES at the O *K*-edge are shown in Fig. 2b for the sample annealed at 700 °C. A strong resonant luminescence, clearly attributable to Tb in the XEOL spectra, is observed.

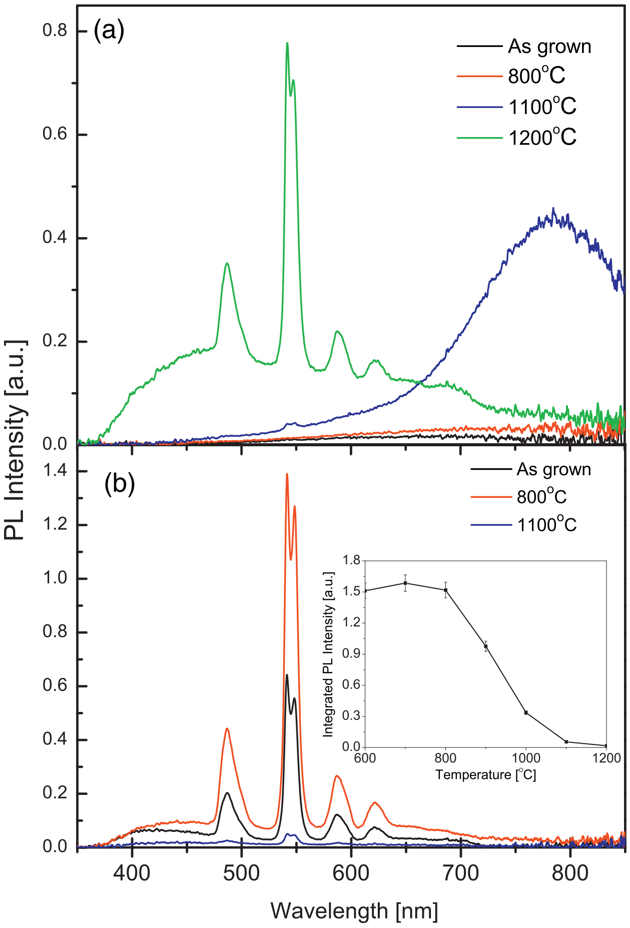

**Figure 1** (online color at: www.pss-b.com) Photoluminescence from Tb-doped (a) SRSO and (b) ORSO thin films annealed at the temperatures shown. The inset in (b) shows the integrated PL intensity as a function of the anneal temperature. In the SRSO film Tb-luminescence is clearly observed only after a 1200 °C anneal. At lower anneal temperatures the PL spectra of the SRSO samples are dominated by Si-nanocluster related emissions. Bright Tb luminescence is observed in the ORSO sample, both as-grown and annealed from 600 to 800 °C. The observed emission lines are characteristic of the $^5D_4 - {}^7F_j$ ($j = 6, 5, 4, 3$) intra-4f transitions of the Tb$^{3+}$ ion. Adapted from Ref. [13].

Figures 3 and 4 show the TEY and PLY XANES for a Tb-doped SRSO film at the Si and O *K*-edges, respectively, annealed at the temperatures shown. Qualitatively, the spectra have similar features to the ORSO film, however, in the as-grown sample no resonant signal is observed in the PLY. Although there appears to be some resonance at the Si–Si edge of the as-grown film, this is largely an artifact of the renormalization of a weak, noisy spectrum, as confirmed by examining the XEOL spectra at this energy. After

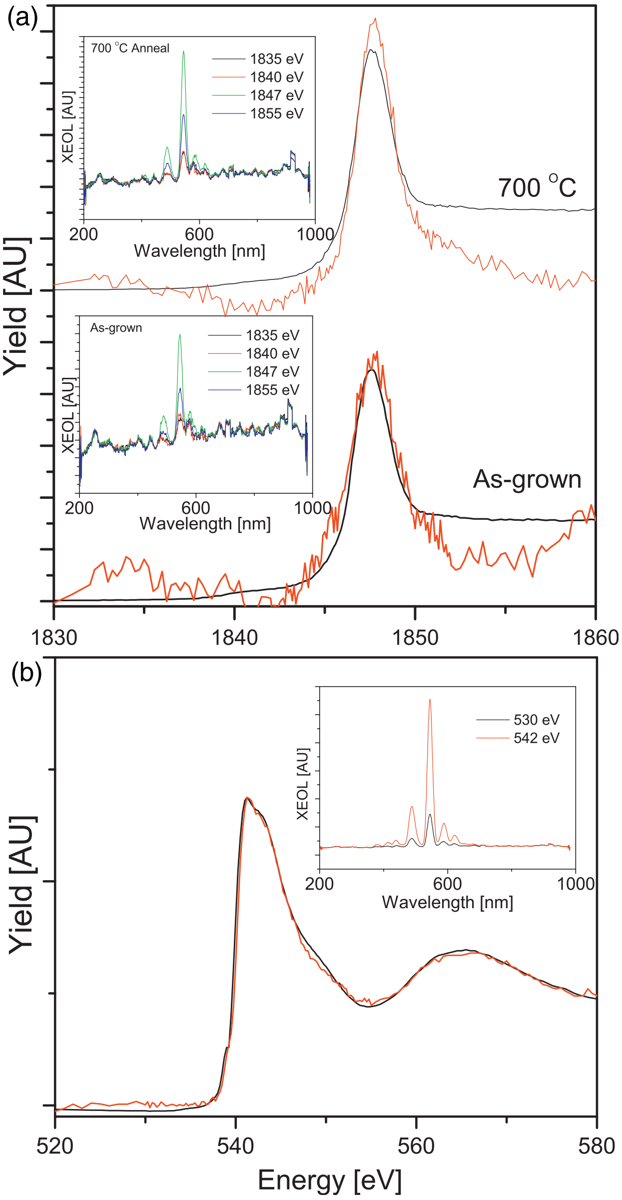

**Figure 2** (online color at: www.pss-b.com) TEY-(black) and PLY-(red) XANES for the Tb-doped ORSO film at (a) the Si *K*-edge for the sample as-grown and annealed at 700 °C and (b) the O *K*-edge after annealing at 700 °C. The insets show the XEOL spectra obtained at the indicated energies. The spectra at 700 °C in (a) have been shifted vertically for clarity.

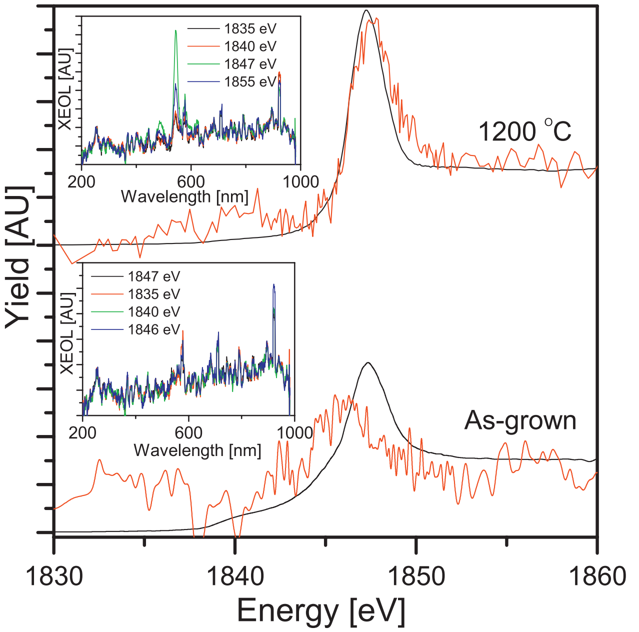

**Figure 3** (online color at: www.pss-b.com) TEY-(black) and PLY-(red) XANES for the Tb-doped SRSO film at the Si *K*-edge and for the sample as-grown and annealed at 1200 °C. The insets show the XEOL spectra obtained at the indicated energies. The spectra at 1200 °C have been shifted vertically for clarity.

annealing at 1200 °C, when Si-ncs are known to have formed in this film and one could expect them to act as sensitizers of the Tb ions, the Tb luminescence nevertheless again is efficiently excited primarily at O-related energies.

In Tb-implanted silicon oxide thin films Tb has been found to exist with two and sixfold coordination to oxygen [26]. As with Er, sixfold coordination of the Tb ion with surrounding oxygen atoms has been found to correspond to the presence of $Tb^{3+}$ luminescence centers [9, 26]. The results discussed here demonstrate, however, that it is not simply a matter of the coordination of Tb with oxygen that leads to luminescence of the Tb ions but rather that the luminescence may be excited through the oxygen bonds themselves. The luminescence of these samples cannot simply be considered a matter of excitation into extended states of the host matrix. Even though such excitation is possible through X-ray absorption, it is, as mentioned above, an unlikely scenario to explain the PL of these samples as they were excited with a 3.81 eV source, well below the bandgap of silicon dioxide. Rather, oxygen related states, either due to defects in the host matrix or oxygen bonding at the Tb sites themselves, are the major contributor to the luminescence of both the ORSO and SRSO samples. An abundance of oxygen in the ORSO film enables the Tb atoms to easily sixfold coordinate with oxygen, and Tb luminescence is observed in the as-grown and low-temperature annealed films. Higher anneal temperatures may lead to the out-diffusion of oxygen from the sample as the silicon oxide submatrix tends towards $SiO_2$. Furthermore, high temperature annealing has been found to lead to Tb clustering, depleting the number of luminescent Tb ions in the film.

The structural make-up of the SRSO film is slightly different as the formation of Si-ncs results in the presence of an additional component contributing to the thermal evolution of these films. At anneal temperatures below 1200 °C primarily Si-nc related PL is observed. Although this PL is a result of the Si-ncs the influence of Si–O bonding (particularly the Si=O double bond) at the Si-nc interface is well known to produce a near infrared emission, as observed. After annealing at 1200 °C, a Tb luminescent signal is observed on a broad background. This background, which is

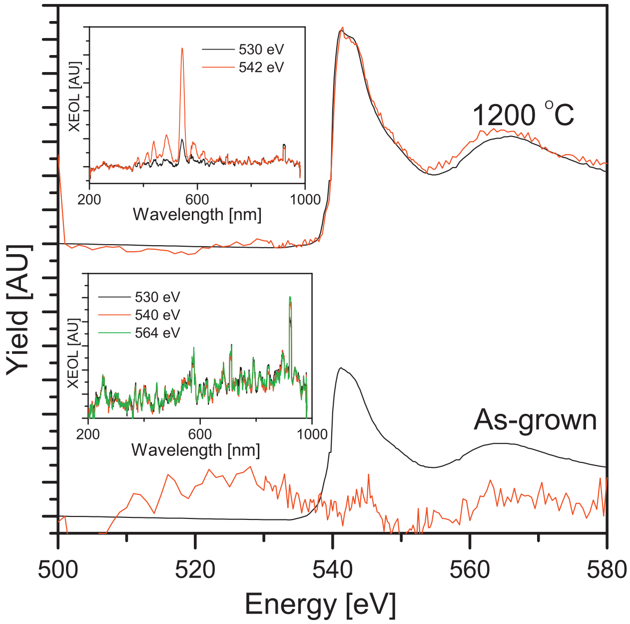

**Figure 4** (online color at: www.pss-b.com) TEY-(black) and PLY-(red) XANES for the Tb-doped SRSO film at the O *K*-edge for the sample as-grown and annealed at 1200 °C. The insets show the XEOL spectra obtained at the indicated energies. The spectra at 1200 °C have been shifted vertically for clarity.

not a feature of Tb luminescence, may be attributed to emission from the Si-ncs themselves or to the formation of oxygen related defects as a consequence of changes in the film structure. The combined growth of the Si-ncs and the breaking of Si=O bonds enables the re-coordination of Tb to the luminescent sixfold structure. Although it has previously been considered that the suppression of the Si-nc PL combined with the enhancement of $Tb^{3+}$ PL is indicative of an energy transfer process occurring between the Si-ncs and the Tb ions, X-ray excitation experiments demonstrate that the Tb luminescence again originates primarily from O-related energy states. The discussed observations for the SRSO samples do not preclude the possibility of Si-ncs acting as sensitizers provided they are resonant with the energy levels of the Tb–O complex. The combined results from XANES and XEOL, however, clearly illustrate that the luminescence process is strongly correlated with an oxygen related chemical environment.

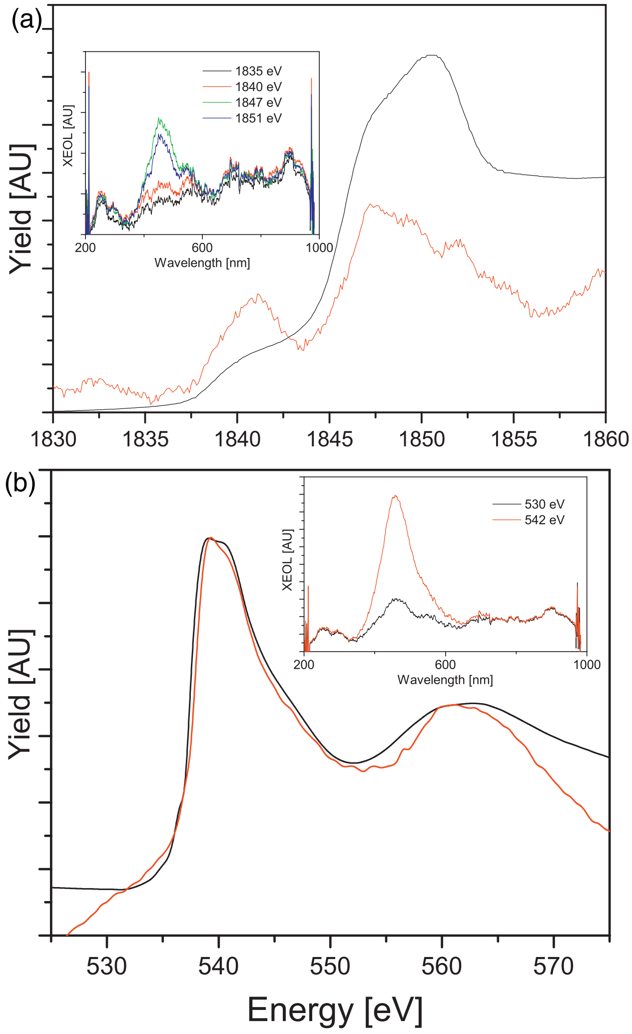

**Figure 5** (online color at: www.pss-b.com) TEY-(black) and PLY-(red) XANES at (a) the Si *K*-edge and (b) the O *K*-edge for the Ce-doped ORSO film annealed at 1200 °C. The insets show the XEOL spectra obtained at the indicated energies.

As with the Tb-doped samples a weak luminescence was observed from the as-grown Ce-doped ORSO samples, increasing in intensity with annealing to 800 °C and then decreasing in intensity at higher anneal temperatures [13]. Unlike the Tb-doped samples, however, a significant increase in the luminescence from the sample was observed after the 1200 °C anneal. This bright luminescence was found to correspond to the formation of a Ce-silicate phase within the films after annealing at this temperature, as confirmed through the use of high-resolution transmission electron microscopy [18]. Figure 5 shows the TEY- and PLY-XANES for this Ce-doped ORSO sample annealed at 1200 °C at the Si and O *K*-edges. In addition to the peaks characteristic of Si–Si and Si–O bonding discussed earlier an additional peak is observed in the TEY-XANES spectrum at 1852 eV. This peak is attributed to Si–Ce bonding in the Ce-silicate phase of the film. In this sample the PLY shows a weak resonance at energies corresponding to Si–Si or Si–Ce bonding. As with the Tb-doped sample, Ce luminescence is strongly resonantly excited at the Si–O peak and at the O *K*-edge. Note that the PLY-XANES decreases in intensity beyond the Si–O peak and does not show a more intense peak at the Si–Ce edge as observed in the TEY-XANES, indicative that XEOL from the sample is, therefore, excited most prominently at O-related energy states and not simply through extended electronic states associated with the host lattice or the silicate phase. O-related energy states then play a similarly significant role for Ce as for Tb in the luminescence of the sample. The weaker resonances of the PLY with the Si–Si and Si–Ce edges demonstrate, however, that the luminescence does not originate from O-related energy states alone. Instead, the incorporation of Ce in the silicate phase leads to Ce–O and Ce–Si bonding, through both of which it is possible to excite the Ce ions to a lesser degree.

**4 Conclusions** Through detailed analysis of their XANES and XEOL spectra the structure and luminescence of Ce- and Tb-doped silicon oxides has been studied and a clear correlation between oxygen related energy states and luminescence has been observed. In a Tb-doped ORSO thin film the ability of Tb ions to easily coordinate with O-atoms in the surrounding host matrix leads to a bright luminescence in the as-grown films, while for the case of an SRSO sample a high temperature anneal is necessary to induce a structural re-ordering of the film – resulting in the formation of Si-ncs and enabling the coordination of Tb with O-atoms in the surrounding host matrix. In a Ce-doped ORSO sample structural re-ordering at high temperatures has been found to lead to the formation of a Ce-silicate phase. Although there is significant structural variation in the films relative to the Tb-doped samples the luminescence of the sample was still strongly correlated with O-related bonding states. A weaker Ce luminescence is also observed at Si–Ce and Si–Si related energies. This behavior is likely associated with the bonding structure of the silicate itself, which enables several luminescent pathways to the Ce ions. Although the microstructure of the films varies from film to film, the results demonstrate that O-related energy states play a significant role in establishing luminescent states in RE-doped silicon oxides. In order to optimize the luminescence of these materials it is, therefore, necessary to consider the local bonding environment of the RE-ions and specific details of electronic states associated with the host matrix.

**Acknowledgements** The authors would like to thank T. K. Sham (University of Western Ontario, London, Ontario, Canada), D. Comedi (Universidad Nacional de Tucumán, Argentina), and the beamline staff at the CLS (R. Blyth, Y. Hu, T. Regier, and L. Zuin) for valuable discussions on synchrotron-based characterization methods and for their assistance in using the CLS facilities. This work has been supported by the Centre for Photonics and the Centre for Materials and Manufacturing, divisions of Ontario Centres of Excellence Inc, and by the Natural Sciences and Engineering Research Council of Canada (NSERC). Part of this work was performed at the CLS synchrotron facility, which is supported by NSERC, CIHR, NRC, and other government agencies.

## References

[1] L. Pavesi and D. J. Lockwood (eds.), Silicon Photonics (Springer, Berlin, 2004).
[2] S. Ossicini, L. Pavesi, and F. Priolo, Light Emitting Silicon for Microphotonics (Springer, Berlin, 2003).
[3] P. M. Fauchet and J. von Behren, Phys. Status Solidi B **204**, R7 (1997).
[4] M. V. Wolkin, J. Jorne, P. M. Fauchet, G. Allan, and C. Delerue, Phys. Rev. Lett. **82**, 197 (1999).
[5] L. Pavesi, L. Dal Negro, C. Mazzoleni, G. Franzo, and F. Priolo, Nature **408**, 440 (2000).
[6] J. Heitmann, M. Schmidt, M. Zacharias, V. Y. Timoshenko, M. G. Lisachenko, and P. K. Kashkarov, Mater. Sci. Eng. B **105**, 214 (2003).
[7] A. J. Kenyon, C. E. Chryssou, C. W. Pitt, T. Shimizu-Iwayama, D. E. Hole, N. Sharma, and C. J. Humphreys, J. Appl. Phys. **91**, 367 (2002).
[8] P. G. Kik and A. Polman, J. Appl. Phys. **88**, 1992 (2000).
[9] A. J. Kenyon, Prog. Quantum Electron. **26**, 225 (2002).
[10] L. Rebohle, J. Lehmann, S. Prucnal, A. Kanjilal, A. Nazarov, I. Tyagulskii, W. Skorupa, and M. Helm, Appl. Phys. Lett. **93**, 071908 (2008).
[11] J. M. Sun, S. Prucnal, W. Skorupa, M. Helm, L. Rebohle, and T. Gebel, Appl. Phys. Lett. **89**, 091908 (2006).
[12] J. M. Sun, W. Skorupa, T. Dekorsy, M. Helm, L. Rebohle, and T. Gebel, J. Appl. Phys. **97**, 123513 (2005).
[13] J. Li, O. H. Y. Zalloum, T. Roschuk, C. L. Heng, J. Wojcik, and P. Mascher, Adv. Opt. Technol. **295601**, 2008 (2008).
[14] T. K. Sham, D. T. Jiang, I. Coulthard, J. W. Lorimer, X. H. Feng, K. H. Tan, S. P. Frigo, R. A. Rosenberg, D. C. Houghton, and B. Bryskiewicz, Nature **363**, 331 (1993).
[15] T. K. Sham, S. J. Naftel, P. S. G. Kim, R. Sammynaiken, Y. H. Tang, I. Coulthard, A. Moewes, J. W. Freeland, Y. F. Hu, and S. T. Lee, Phys. Rev. B **70**, 045313 (2004).
[16] D. Comedi, O. H. Y. Zalloum, D. E. Blakie, J. Wojcik, and P. Mascher, ECS Trans. **3**, 3 (2006).
[17] T. K. Sham and R. A. Rosenberg, Chem. Phys. Chem. **8**, 2557 (2007).
[18] J. Li, O. H. Y. Zalloum, T. Roschuk, C. L. Heng, J. Wojcik, and P. Mascher, Appl. Phys. Lett. **94**, 011112 (2009).
[19] M. Boumerzoug, Z. D. Pang, M. Boudreau, P. Mascher, and J. G. Simmons, Appl. Phys. Lett. **66**, 302 (1995).
[20] O. H. Y. Zalloum, M. Flynn, T. Roschuk, J. Wojcik, E. Irving, and P. Mascher, Rev. Sci. Instrum. **77**, 023906 (2006).
[21] T. Regier, J. Paulson, G. Wright, I. Coulthard, K. Tan, T. K. Sham, and R. I. R. Blyth, AIP Conf. Proc. **879**, 473 (2007).
[22] T. Regier, J. Krochak, T. K. Sham, Y. F. Hu, J. Thompson, and R. I. R. Blyth, Nucl. Instrum. Methods Phys. Res. A **582**, 93 (2007).
[23] M. Kasrai, W. N. Lennard, R. W. Brunner, G. M. Bancroft, J. A. Bardwell, and K. H. Tan, Appl. Surf. Sci. **99**, 303 (1996).
[24] H. Jeong, S.-Y. Seo, and J. H. Shin, Appl. Phys. Lett. **88**, 161910 (2006).
[25] N. Daldosso, G. Das, S. Larcheri, G. Mariotto, G. Dalba, L. Pavesi, A. Irrera, F. Priolo, F. Iacona, and F. Rocca, J. Appl. Phys. **101**, 113510 (2007).
[26] H. Ofuchi, Y. Imaizumi, H. Sugawara, H. Fujioka, M. Oshima, and Y. Takeda, Nucl. Instrum. Methods Phys. Res. B **199**, 231 (2003).